Molecular Dynamics Simulation for Monolayers of Alkyl Thiol Molecules at Air-Solid Interfaces

Song Hi Lee* and Han Soo Kim†

Department of Chemistry, Kyungsung University, Pusan 608-736, Korea
†Department of Industrial Chemistry, Kangnung National University, Kangnung 212-702, Korea
Received February 29, 1996

We present the results of molecular dynamics simulations of monolayers of long-chain alkyl thiol [$S(CH_2)_{15}CH_3$] molecules on an air-solid interface using the extended collapsed atom model for the chain-molecule and a gold surface for the solid surface. Several molecular dynamics simulations have been performed on monolayers with areas per molecule ranging from 18.30 to 32.10 A^2/molecule. It is found that there exist three possible transitions: a continuous transition characterized by a change in molecular configuration without change in lattice structure, a sudden transition characterized by the distinct lattice defects and perfect islands, and a third transition characterized by the appearance of a random, liquid-like state. The analysis of probability distributions of the segments shows that the structure of the chain-molecules at the air-solid interface is completely different from that at the air-water interface in the view of the degree of overlap of the probability distributions of the neighbor segments. The calculated diffusion coefficients of the chain-molecules on the monolayers seem to be not directly related to any one of the three transitions. However, the large diffusion of the molecules enhanced by the increment of the area per molecule may induce the second transition.

Introduction

Self-assembled monolayers of long-chain molecules in a variety of interfaces have been a popular subject of study over the years experimentally and theoretically. The preparation and structural characterization of supported monolayer assemblies of oriented chain-molecules has broad potential applications. Examples involve lubrication,[1] electrochemistry,[2,3] electronic and vibrational spectroscopy,[4,5] photochemical mechanisms,[4,6] electrical conduction,[4,7] catalysis,[8] and biological membranes.[9] There is also an interesting but rather complex body of investigations of films that have been deposited on solid supporting surfaces.

Computer simulation methods are useful to investigate complex physical systems, to test theoretical models, and to compare experimental results. Molecular dynamics simulations are especially suitable for the study of dynamic properties such as time-correlation functions. There have been many attempts to use molecular dynamics (MD), Monte Carlo (MC), and Brownian dynamics (BD) methods to investigate the structure of Langmuir monolayers over the last few years. These have resulted in a growing understanding of structure and dynamics of real, complex systems such as Langmuir monolayers and multilayers,[10-12] biological membranes,[13,14] surface adsorbed chain-molecules[15,16] and molecular/liquid crystals of chain-molecules.[17,18]

Experiments showed that long-chain alkyl thiols form films that are thermally more stable than films formed from short-chain alkyl thiols, and that monolayers of alkyl thiol molecules on gold appear to be stable indefinitely at room temperature but their constituents desorb when heated.[19] To try to understand these experimental results, Hautman and Klein reported molecular dynamics simulations for the system of alkyl thiol molecules [$S(CH_2)_{15}CH_3$] on a gold surface.[20,21] Firstly they calculated the structure and dynamics for two different models at a fixed surface density and room temperature. The principal difference between the two models is the initial orientation of the first S-C bond: in one the orientation of the first bond with respect to the surface normal is unrestricted, while the other leaves the angle, θ_0, between the S-C bond and the surface normal, subject to a harmonic bending potential. The results calculated by them showed that the thickness of monolayers is not largely dependent on the tilt angle, but there are striking differences in the chain rotational dynamics of the two models. In their system, the S-C and C-C bond lengths and the S-C-C and C-C-C bond angles are kept constant without considering bond stretching and bond angle bending interactions. Secondly they studied the effect of temperature on a dense monolayer of [$S(CH_2)_{15}CH_3$]. It revealed that the orientation of the chain-molecules is entirely dependent on the temperature of the system. Also nonequilibrium molecular dynamics techniques were used to investigate the transition from the disordered state to the orientationally ordered state.

In this paper, we investigate the structures and thermodynamics of monolayers of long-chain alkyl thiol molecules on an air-solid interface as a function of area per molecule, using molecular dynamics simulation method, especially, to study the phase transition in the monolayer, the fraction of *trans* formation, the thickness of the monolayer, monolayer tilting, lattice defects, and diffusion of the chain molecules. Also additional studies of how the area per molecule of chain-molecules in the surface affects the characterization of Langmuir monolayer is carried out. The solid surface is modeled by the gold surface as in the studies of Klein *et al.*[20,21] Bareman and Klein already carried out molecular dynamics calculations to investigate the collective molecular tilt as a function of area per molecule at room temperature in substrate-supported monolayers of long-chain molecules at the air-solid interface.[22] The results obtained in their work showed that the collective tilt angle was increased continuously as the area per molecule was increased without

any significant effect on the phase transition. However, the range of areas per molecule studied by them (18-24 Å^2/molecule) is smaller than the range studied by Toxvaerd *et al.* (18-32 Å^2/molecule).[23,24]

The monolayer tilt has been a subject of great controversy over the last few years, and the role played by the tilt angle in the phase transition is still unknown. More recently, Toxvaerd *et al.* performed molecular dynamics simulations on Langmuir monolayers of linear chain surfactants at the air-water interface, using two different configurations of the solid phase-a rectangular unit cell monolayer and a hexagonal unit cell monolayer.[23,24] They found two transitions in the monolayer as a function of area per molecule-a continuous transition characterized by a change in chain conformation and a first-order phase transition characterized by a sharp rise in lattice defects and chain diffusion. They also reported that structure factor results and other order parameters indicate no significant shape dependence.

Molecular dynamics simulations of liquid-supported monolayers of perfluorinated and partially fluorinated amphiphiles were studied by Rice *et al.*.[25~28] First they reported that the observed breakup of the homogeneous ordered monolayer into ordered islands with the same collective tilt of the chain molecules is correctly predicted but the experimental and simulation values of the tilt angles were not in quantitative agreement. Later the discrepancy between the predicted and observed tilt angles was removed by including the effect of the azimuthal distribution of individual molecular tilt angles.

In the present work, we follow the molecular dynamics simulation methods of Toxvaerd *et al.*.[23,24] The main purpose of this work is three-fold: first, we extend the work done by Klein *et al.*[22] to a wide range of area per molecule to see further changes as a function of area per molecule. Second, the phase transition observed in the monolayer of long-chain molecules at the air-water interface as a function of area per molecule[23,24] is examined for monolayer of long-chain molecules at the air-solid interface. Third, the structure and thermodynamics of monolayers of long-chain alkyl thiol molecules on the air-solid interface as a function of area per molecule are investigated. We also consider the bond stretching interaction and the bond angle bending interaction for the intramolecular interactions.

This paper is organized as follows. In Sec. II, the details of the molecular model and molecular dynamics simulation method in a NVT ensemble are presented. We discuss our simulation results of monolayers of long-chain alkyl thiol molecules in the air-solid interface in Sec. III and present the concluding remarks in Sec. IV.

Molecular Model and Molecular Dynamics Simulation Methods

Molecular Model. The systems studied in this work consist of 90 surfactant chain-molecules periodically replicated in the x- and y-directions. The chain-molecules considered here make up a sulfur head-group, 15 methylene segments, and a methyl tail-group. The molecular model used for the chain-molecules is the so-called extended collapsed atom model, developed by Chynoweth *et al.*,[29] in which monomeric units (sulfur atom, methylene, or methyl) are typically treated as a single sphere (or site) with a Lennard-Jones (LJ) potential between the spheres. Not only sites on different chain-molecules but sites more than three apart on the same chain-molecule interact through a 12-6 LJ potential. In Ryckaert and Bellemans' original collapsed atom model,[30] a C-C-C-C torsional rotation potential is also included.

The interaction between each site and the solid surface is given by a 12-3 LJ potential which have the form of[20,21]

$$V(z)=\frac{C_{12}}{(z-z_0)^{12}}-\frac{C_3}{(z-z_0)^3} \tag{1}$$

where z is the distance between each site and the surface, and C_{12}, C_3, and z_o are fitting potential parameters which are given in Table 1 for the several different sites.

Bond stretching interaction between adjacent sites on the same chain are also considered.[31] The potential energy associated with bond stretching between sites i and j is assumed to be harmonic and is given by

$$V_s=k_s(|r_{ij}|-r_e)^2 \tag{2}$$

Here, r_{ij} is the bond vector, r_e is the equilibrium distance and k_s is the force constant (the last two are constant parameters depending upon the type of sites i and j only). F_{ij} is obtained from the derivative of the potential with respect to the coordinate of site i, and is given by

$$F_{ij}=-2k_s(|r_{ij}|-r_e)\ \frac{r_{ij}}{|r_{ij}|} \tag{3}$$

Bond angle bending denotes the interaction between three consecutively bonded sites i, j and k. The potential energy associated with bond angle bending is also harmonic and is given by

$$V_b(\theta)=k_b(\theta-\theta_o)^2 \tag{4}$$

where θ is C-C-C or S-C-C angle, θ_0 is the equilibrium bond angle, and k_b are the force constant (the last two are constant parameters depending upon the type of sites i, j and k only). The force on each site is a pseudo-pairwise force obtained by differentiation[32] and,

$$\begin{aligned} F_{ij}&=\frac{1}{|r_{ij}|}\ \frac{dV_b}{d\theta}\ \frac{r_{ij}\times(r_{kj}\times r_{ij})}{|r_{ij}\times(r_{kj}\times r_{ij})|},\\ F_{kj}&=\frac{1}{|r_{kj}|}\ \frac{dV_b}{d\theta}\ \frac{r_{kj}\times(r_{ij}\times r_{kj})}{|r_{kj}\times(r_{ij}\times r_{kj})|},\\ F_{ik}&=0 \end{aligned} \tag{5}$$

where r_{ij} and r_{kj} are the two bond vectors, and $dV_b/d\theta$ is derived analytically from Eq. (4).

The changes in the equilibrium dihedral angles are subject to torsional rotational potential. Torsional rotation about a bond denotes the bonded interaction between four sites i, j, k and l. The potential energy associated with torsional rotation is represented by the original Ryckaert-Bellemans potential[30]

$$\begin{aligned} V_t(\psi)=&a_0+a_1\cos(\psi)+a_2\cos^2(\psi)\\ &+a^3\cos^3(\psi)+a_4\cos^4(\psi)+a_5\cos^5(\psi) \end{aligned} \tag{6}$$

where ψ is the dihedral angle. The corresponding forces are

$$F_n=-\frac{dV_t}{d\cos\psi}\ A_n, \tag{7}$$

Table 1. Potential parameters for $S(CH_2)_{15}CH_3$ molecule

Bond stretching		S-C	C-C		
r_e (nm)		0.182	0.153		
k_s (kJ/mol·nm^2)		132600	132600		
Bond angle bending		S-C-C	C-C-C		
θ_o (deg)		109.5	114.4		
k_b (kJ/mol·deg^2)		0.07915	0.07915		
L-J 12-6 potential		S	CH_2	CH_3	
σ (nm)		0.425	0.3905	0.3905	
ε (kJ/mol)		1.6629	0.4939	0.7325	
L-J 12-3 potential		S	CH_2	CH_3	
z_o (nm)		0.0269	0.086	0.086	
C_{12} (10^7 kJ/mol)		3.3998	2.3280	2.8352	
C_3 (kJ/mol)		1.5016	0.1422	0.1729	
Torsional potential (kJ/mol)					
a_1	a_2	a_3	a_4	a_5	a_6
9.279	12.156	−13.120	−3.060	26.240	−31.495

where $dV_t/d\cos\omega$ is derived analytically from Eq. (7) and the Ars are given by[32]

$$A_{ij}=\frac{r_{kj}\times(r_{ik}\times r_{kj})}{|r_{ij}\times r_{kj}||r_{kj}\times r_{ik}|}-\frac{r_{kj}\times(r_{ij}\times r_{kj})\cos\psi}{|r_{ij}\times r_{kj}|^2},$$

$$A_{ik}=\frac{r_{kj}\times(r_{ij}\times r_{kj})}{|r_{ij}\times r_{kj}||r_{kj}\times r_{ik}|}-\frac{r_{kj}\times(r_{ik}\times r_{kj})\cos\psi}{|r_{ik}\times r_{kj}|^2}, \quad (8)$$

$$A_{kj}=\frac{r_{ij}\times(r_{ik}\times r_{kj})}{|r_{ij}\times r_{kj}||r_{kj}\times r_{ik}|}-\frac{r_{ij}\times(r_{ij}\times r_{kj})\cos\psi}{|r_{ij}\times r_{kj}|^2},$$

$$+\frac{r_{ij}\times(r_{ij}\times r_{kj})}{|r_{ij}\times r_{kj}||r_{kj}\times r_{ik}|}-\frac{r_{ik}\times(r_{ik}\times r_{kj})\cos\psi}{|r_{ik}\times r_{kj}|^2},$$

$$A_{ik}=A_{ii}=A_{jj}=0$$

in which r_{ij}, r_{kj}, r_{ik} are the three bond vectors. The potential parameters-r_e, k_s, θ_0, k_b, a_0, a_1, a_2, a_3, a_4, and a_5-used in our study are given in Table 1.

Molecular dynamics simulation in a canonical ensemble. In the present work, a canonical ensemble of fixed N (=90 chain-molecules), V (=volume of rectangular box), and T (=293.15 K) is chosen for the simulation ensemble. In this ensemble, 13 monolayers of chain-molecules are selected and the areas per molecule range from 18.30 to 32.10 Å^2/molecule. The preliminary molecular dynamics simulation of monolayer of the chain-molecules is started from a compressed state at 21.39 Å^2/molecule with the head-group being on the lattice point of a regular hexagonal structure of the solid surface. The lengths of the simulation box are XL=4.473, YL=4.304, and fixed ZL=2.023 nm. In order to simulate smaller or larger area per molecule of monolayers, the box size is periodically increased or decreased in the x- and y-directions. For the initial configurations of all the chain-molecules, the orientation of the first S-C bond with respect to the surface normal is unrestricted, the sulfur head group is located at the lattice point of a regular hexagonal structure, 0.24 nm apart from the solid surface, and the consecutive methylene and methyl sites are placed in the z-direction so that the bond length and the bond angles are kept at 0.153 nm and 109.5° respectively.

Gauss's principle of least constraint[33] is used to maintain the system at the constant temperature. The ordinary periodic boundary condition in the x- and y-directions only and minimum image convention for the LJ potential are applied with a spherical cut-off distance of radius 0.9808 nm. Gear's fifth order predictor-corrector method[34] is employed for time integration algorithm with time step of 0.5 fs (femto second). Each simulation is equilibrated for approximately 200,000 time steps (100 ps), and followed by 10,000 time steps (50 ps) for sampling. The trajectories (configurations and orientations) of the chain-molecules are stored every ten time steps (5 fs).

Table 2. Average potential from our molecular dynamics simulations for monolayers of $S(CH_2)_{15}CH_3$

Area/ molecule (Å^2)	L-J potential energy (kJ/mol)	Dihedral energy	C-C bond stretching energy	C-C-C bond angle bending energy
18.30	−123.9	0.995	10.58	14.70
19.30	−123.5	1.043	16.16	15.72
20.33	−119.2	1.176	11.44	15.82
21.39	−119.0	1.108	7.16	15.24
22.47	−113.7	1.182	12.72	15.94
23.58	−108.6	1.357	19.76	17.38
24.72	−109.6	1.284	13.67	16.09
25.88	−105.4	1.322	16.69	16.75
27.07	−105.4	1.372	10.60	16.22
28.29	−103.4	1.394	12.25	16.28
29.53	−105.2	1.319	9.73	15.63
30.80	−102.0	1.392	20.60	17.32
32.10	−99.5	1.547	11.32	16.45

Results

Thermodynamics. Several potential energies calculated from our molecular dynamics simulations are given in Table 2. Both LJ potential and torsional energies are almost monotonically increased with increasing area per molecule, but C-C bond stretching and C-C-C bond angle bending energies are rather constant with large variance. These results do not provide any clue to the relationship between conformational transition and the change of area per molecule.

Structure. Chain conformation results from our molecular dynamics simulations for monolayers of $S(CH_2)_{15}CH_3$ are listed in Table 3. First, the values of head-to-end distance and monolayer thickness are plotted as a function of area per molecule in Figure 1. The head-to-end distance is directly related to the fraction (%) of *trans* bond and decreases monotonically, except at 29.53 Å^2/molecule, as the area per molecule is increased. The fraction of *trans* bond shows exactly the same trend as shown in Figure 2. However, the behavior of monolayer thickness is rather complicated-it goes up, down, up, and down. Although the monolayer thickness is related to both the fraction of *trans* bond and the monolayer tilt angle, it is insensitive to the fraction of *trans* bond since it decreases almost monotonically with very little variance. Hence, the main factor of the monolayer thickness is the monolayer tilt angle.

The monolayer tilt angle is sensitive to the change of the area per molecule. It is simply calculated from the monolayer thickness, l:

Table 3. Chain conformation results from our molecular dynamics simulations for monolayers of $S(CH_2)_{15}CH_3$ and diffusion coefficients (10^{-5} cm^2/sec) of the chain-molecules

Area/molecule (Å^2)	Head-to-tail distance	Monolayer thickness	*Trans* Bond Fraction (%)	Tilt Angles Eq. (9)	Tilt Angles Eq. (10)	Diffusion coefficients
18.30	2.011	1.866	99.97	22.69	21.60	0.0356
19.30	2.009	1.857	99.74	23.34	22.33	0.0515
20.33	2.004	1.847	99.10	24.04	22.42	0.0814
21.39	2.000	1.732	99.05	31.09	29.49	0.1049
22.47	1.997	1.724	98.76	31.53	29.91	0.1129
23.58	1.980	1.705	97.00	32.54	30.02	0.1165
24.72	1.974	1.714	96.70	32.06	29.45	0.5173
25.88	1.963	1.720	96.21	31.74	26.78	0.5345
27.07	1.941	1.851	95.11	23.77	13.42	0.6173
28.29	1.914	1.830	94.46	25.20	3.89	0.6801
29.53	1.942	1.848	95.45	23.98	10.67	0.7414
30.80	1.900	1.821	94.57	25.79	8.61	0.7969
32.10	1.876	1.710	92.51	32.28	15.11	0.9832

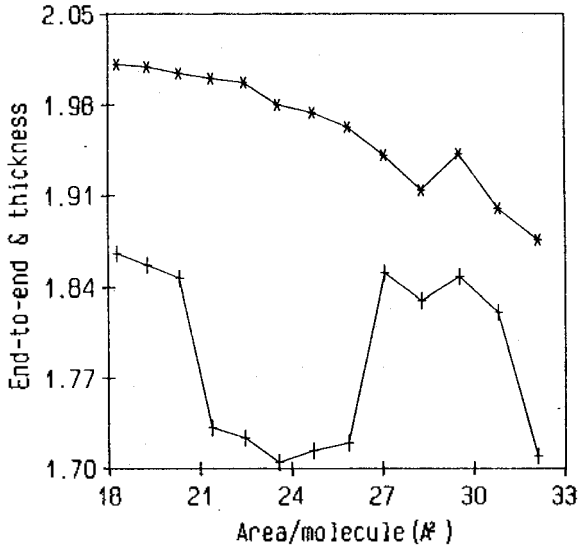

Figure 1. The head-to-tail distance (*) and the monolayer thickness (+) as a function of area per molecule.

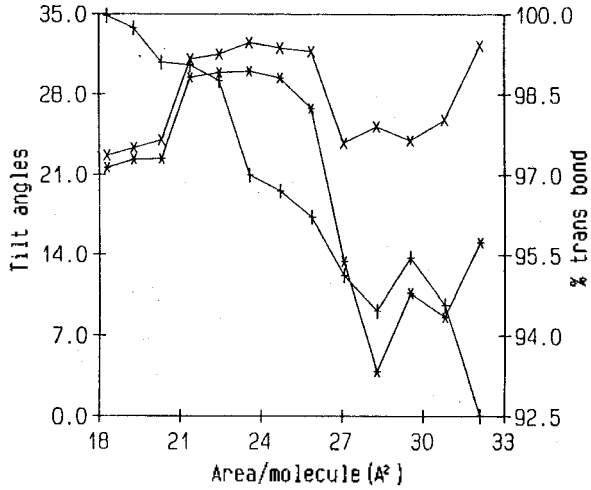

Figure 2. The fraction (%) of *trans* bond (+) and the tilt angles (x and *) calculated from Eqs. (9) and (10) as a function of area per molecule.

$$\cos\theta = l/l_t, \tag{9}$$

where l_t is the thickness of a completely *trans* and upright monolayer. Another way to calculate the tilt angle is through the average of the tilt of all molecules

$$\cos\theta = \frac{1}{N}\sum_{i=1}^{i=N}\frac{\vec{u}_i\cdot\vec{u}_n}{|\vec{u}_i||\vec{u}_n|} \tag{10}$$

where N is the total number of molecules, $\vec{u}_i$ is the vector that corresponds to the highest eigen value in the moment of inertia tensor, and $\vec{u}_n$ is the vector normal to the monolayer interface.

The tilt angles calculated from Eqs. (9) and (10) as a function of area per molecule are shown in Figure 2. Both tilt angles show the same trend over all the areas per molecule with large variance after 27.07 Å^2/molecule and the comparison of these angles indicates that Eq. (9) overestimates the monolayer tilt since it assumes the absence of any *gauche* defects in the chain. That is why the behavior of the tilt angle from Eq. (9) is more similar to that of the monolayer thickness than Eq. (10). The tilt angle distribution changes significantly between 20.30 and 21.37 Å^2/molecule and 25.88 and 27.07 Å^2/molecule, which implies some kinds of transitions between them.

These results for the tilt angles are entirely different from previous studies of Toxvaerd *et al.*[23,24] for Langmuir monolayers of linear chain surfactants at the air-water interface, in which the calculated tilt angles from Eqs. (9) and (10) monotonically increased from 3° to 22° and from 10° to 38° respectively with increasing area per molecule (18.5-30 Å^2/molecule). Notice however that our system is at the air-solid interface. The average fraction (%) of *trans* bond over 14 dihedral angles on the chain molecule decreases monotonically except at 29.53 Å^2/molecule as the area per molecule is increased as shown in Figure 2.

The snapshots in Figure 3, which are projections of the molecular configurations onto the xy plane, display the final configuration of each simulation at six different areas per molecule. Figure 3(a) and 3(b) show the tilting structure of the chain

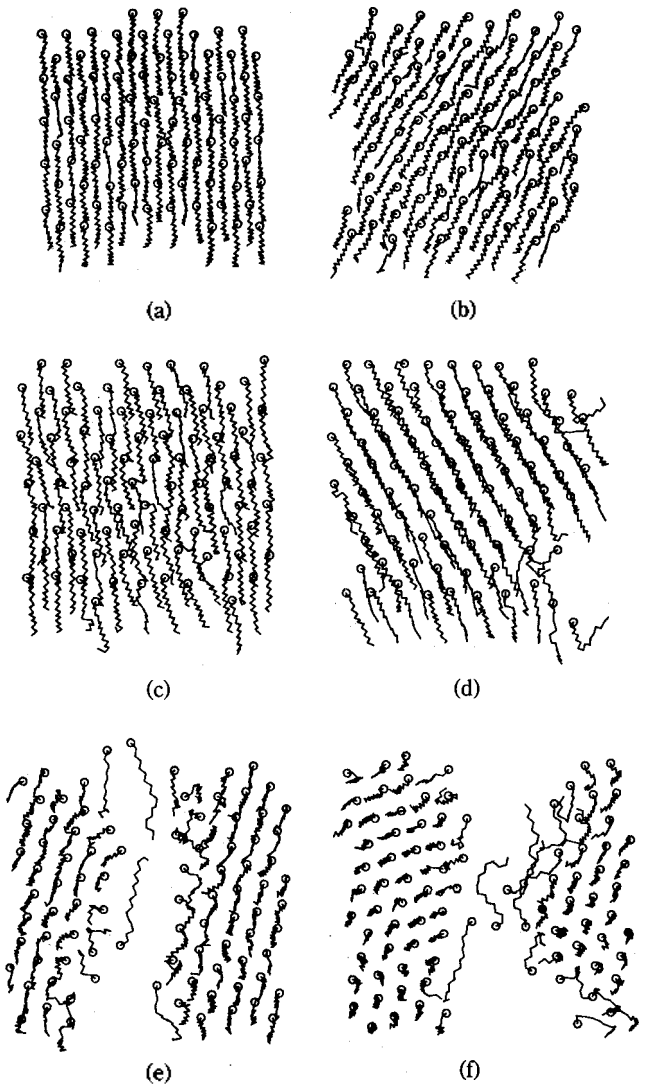

Figure 3. Snapshots (projections onto the xy plane) of the final configurations of the chain-molecules of each simulation at six different areas per molecule: (a) 18.30, (b) 20.30, (c) 22.47, (d) 24.72, (e) 27.07, and (f) 29.53 A^2/molecule.

molecules in the monolayer at 18.30 and 20.33 A^2/molecule, respectively. The head-groups form nearly regular hexagonal structures, not changed from those of the initial configurations. These molecules tend to change the direction of the tilting in concert without significant change in the thickness or the tilt angle of the monolayer (see Figures 1 and 2) as the area per molecule increases from Figure 3(a) to 3(b) because the molecules reorient toward the more stable configuration in energetics. In Figure 3(c) and 3(d), the tilting of the molecules is enhanced by the increment of the area per molecule. This results in sudden change of the thickness and the tilt angles from the monolayer at 20.33 to that at 21.39 A^2/molecule as shown in Figures 1 and 2. However, the snapshots in Figure 3(b) and 3(c) look not much different and the transition from Figure 3 (b) to (c) is characterized by a continuous change in molecular configuration without change in lattice structure. This kind of transition is already reported by Toxvaerd *et al.*[23,24] but the interfaces are different, that is, the air-water and the

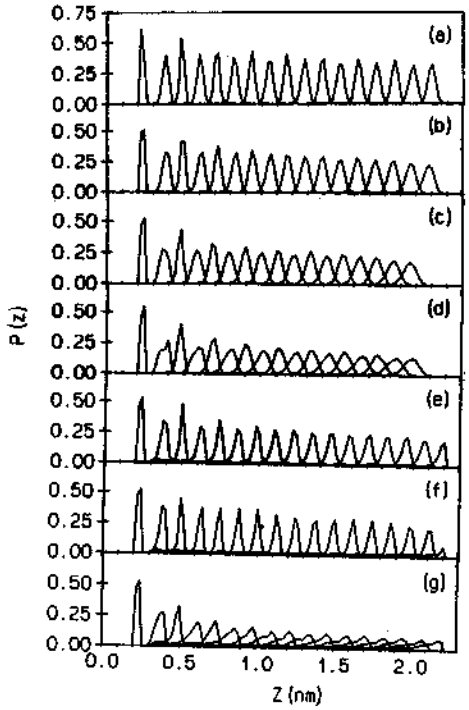

Figure 4. The probality distribution of segments, P(z), at seven different areas per molecule: (a) 18.30, (b) 20.30, (c) 22.47, (d) 24.72, (e) 27.07, (f) 29.53, and (g) 32.10 A^2/molecule.

air-solid interfaces.

It is seen in particular, from Figure 3(d) at 24.72 A^2/molecule, that the breakup of the ordered monolayer begins with the appearance of the lattice defect on the hexagonal structure at the right bottom corner in the figure. Figures 3(e) and 3(f) show clearly that the monolayer breaks up into islands. The interaction between the methylene sites and the solid surface becomes important due to blank spaces of the islands, and the chain-molecules near the islands come closer to the solid surface. The chain-molecules beyond the islands rather tend to straighten up. A similar result is found in the other molecular dynamics simulation of liquid-supported monolayers of perfluorinated and partially fluorinated amphiphiles.[26] Because the breakup of ordered monolayers is possible through the lattice defects, the phase of Figure 3(d) is completely different from that of Figure 3(e). In Figure 3(d) only the lattice defects begin to appear, but in Figures 3(e) and 3(f) not only the lattice defects but perfect islands of the monolayer are seen. The transition from Figure 3(d) to 3(e) is characterized by the distinct lattice defects and the appearance of perfect islands.

In Figure 4, we show the probability distributions of segments normal to the interface for seven different area per molecule which are the primary measurers of locai structure. The singlet probability $P_i(z)$ can be determined directly from our molecular dynamics simulations by

$$P_i(z)=\frac{\langle N_i(z)\rangle}{N} \tag{11}$$

where N is the total number of molecules, and $\langle N_i(z)\rangle$ is the average over time of the number of segments i that are found in a slab of thickness Δz with distance z from the $z=0$ plane. Δz used in all simulations was equal to 0.02 nm.

The results calculated in this system are completely different from those by Toxvaerd *et al.*[23,24] in the view of the large degree of overlap of distributions of the neighbor segments. This reflects the main difference between the air-solid and the air-water interfaces. The translational motion of the chain-molecules at the air-solid interface in the direction normal to the surface is restricted within very narrow limits since the head segment always shows the same height and fixed location of distribution through all the areas per molecule which reflects a strong interaction between the head group and the solid surface. The probablity distributions in Figure 4(a) and 4(b) are similar and are spaced equally on the surface normal with small changes in the distribution heights. But in Figure 4(c) and 4(d) almost all the segments show low, varying heights and broad, unequally spaced distributions with overlap of them. The figure also shows the continuous change in molecular configuration without change in lattice structure (Figure 4(b) to 4(c)) corresponding to the change from Figure 3(b) to 3(c). Conversely in Figure 4(e) and 4(f), the heights of the peaks are increased, and the widths become rather equally spaced and sharp with the disappearance of the overlap of distributions. This signals a sudden change in molecular configuration with a possible change in lattice structure-the presence of distinct lattice defects and perfect islands. Finally in Figure 4(g), the probablity distributions have very broad peaks with the increasing width of the segments closer to the tail. This implies that there exists a third transition from Figure 4(f) to 4(g) characterized by the appearance of a random, liquid-like state.

Dynamics. The mean square displacement (MSD) of the centers-of-mass, the head groups, and the tail groups of the alkyl thiol molecules at two areas per molecule (24.72 and 29.53 A^2/molecule) are shown in Figure 5 and the translational diffusion coefficient of the molecule in the monolayer is calculated for the center-of-mass from the mean square displacement using the equation

$$D = \lim_{t\to\infty} \frac{\langle r^2(t)\rangle}{4t} \tag{12}$$

$$\text{where } r^2(t) = \frac{1}{N}\sum_{i=1}^{N} ([x_i(t)-x_i(0)]^2 + [y_i(t)-y_i(0)]^2) \tag{13}$$

The diffusion coefficients of the centers-of-mass of the alkyl thiol molecules as a function of area per molecule are given in Table III and plotted in Figure 6, while those of the head and tail groups of the molecules are not obtained because of the non-linear MSD of them. The diffusion coefficients plotted in Figure 6 show a monotonic increment with increasing area per molecule with a rapid jump between 23.58 and 24.72 $Å^2$/molecule. This region corresponds neither to the continuous change in molecular configuration without change in lattice structure (Figure 3(b) to 3(c)) nor to the change caused by the distinct lattice defects and perfect islands (Figure 3(d) to 3(e)), but it corresponds to the changes shown from Figure 3(c) to 3(d).

It is worth noting that the breakup of the ordered monolayer begins at 24.72 $Å^2$/molecule (Figure 3(d)). The large diffusion of the molecules enhanced by the increment in the area per molecule may induce the appearance of the lattice defect on the hexagonal structure followed by the transition characterized by the distinct lattice defects and perfect islands. However, the linearity of the 3-4 strands of molecules lying down near the lattice islands shown in Figure 3(e) remains unexplained except perhaps to indicate a metastable structure of the close-packed monolayer inside the cluster manifested by the very small tilt angle and small molecular separation of the molecules lying down on the surface due to the decreased area per molecule.

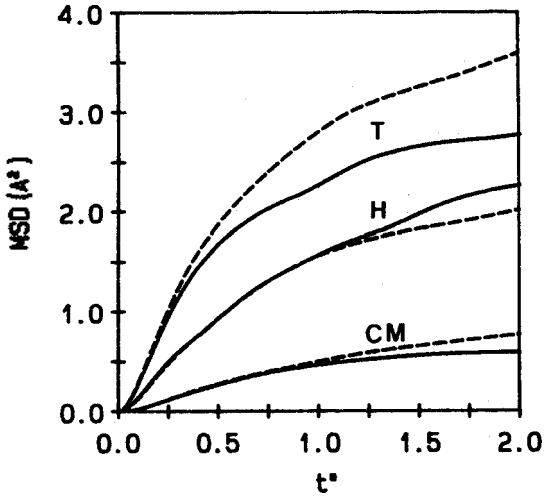

Figure 5. The mean square displacement (MSD) of the alkyl thiol molecules at two different areas per molecule: — for 24.72 and ··· for 29.53 A^2/molecule. H, T, and CM represent the head group, the tail group, and the center-of-mass of the molecules, respectively.

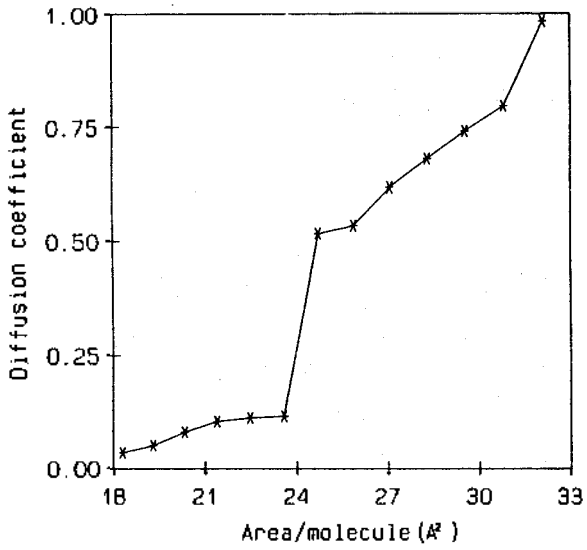

Figure 6. The diffusion coefficients of the alkyl thiol molecules calculated from MSD as a function of area per molecule.

Conclusion

Molecular dynamics simulations have been applied to the study the structures and thermodynamics of monolayers of long-chain alkyl thiol [$S(CH_2)_{15}CH_3$] molecules on an air-solid interface as a function of area per molecule. The results reveal three possible transitions: a continuous transition characterized

by a change in molecular configuration without change in lattice structure, a sudden transition characterized by the distinct lattice defects and perfect islands, and a third transition characterized by the appearance of a random, liquid-like state. The analysis of probability distributions of the segments shows that the structure of the chain-molecules at the air-solid interface is completely different from that at the air-water interface in the view of the high degree of overlap of the probability distributions of the neighbor segments. The calculated diffusion coefficients of the chain-molecules on the monolayers seem to be not directly related to any one of the three transitions. However, the large diffusion of the molecules enhanced by the increment of the area per molecule may induce the second transition.

Acknowledgment. This work was supported by a research grant to SHL from the Research Foundation of Kyungsung University. The authors thank to the Computer Center at Korea Institute of Science and Technology for the access to the Cray-C90 system.

References

1. Adamson, A. W. *Physical Chemistry of Surfaces*, 3rd ed.; Wiley: New York, 1976; Chapter 10.
2. Murray, R. W. *Acc. Chem. Res.* **1980**, *13*, 135.
3. (a) Soriaga, M. P.; Hubbard, A. T. *J. Am. Chem. Soc.* **1982**, *104*, 3937. and references therein. (b) Hubbard, A. T. *Acc. Chem. Res.* **1980**, *13*, 177.
4. Kuhn, H.; mobius, D. In *Techniques of Organic Chemistry*; Weisssberger, A.; Rossiter, B. W., Eds.; Wiley: New York, 1972; Vol. 1, Chapter 7.
5. (a) Knoll, W.; Philpott, M. R.; Golden, W. G. *J. Chem. Phys.* **1982**, *77*, 219. (b) Rabolt, J. F.; Santo, R.; Swalen, J. D. *Appl. Spectrosc.* **1980**, *34*, 517.
6. Whitten, D. G. *Angew. Chem., Int. Ed. Engl.* **1979**, *18*, 440.
7. (a) Polymeropoulos, E. E.; Sagiv, J. *J. Chem. Phys.* **1978**, *69*, 1836. (b) Sugi, M.; Fukui, T.; Lizima, S. *Phys. Rev.* **1978**, *B18*, 725. (c) Furtlehner, J. P.; Messiner, J. *Thin Solid Films* **1980**, *68*, 233.
8. Richard, M. A.; Deutsch, J.; Whitesides, G. M. *J. Am. Chem. Soc.* **1979**, *100*, 6613.
9. (a) Waldbilling, R. C.; Robertson, J. D.; McIntosh, T. J. *Biochim. Phiophys. Acta* **1976**, *448*, 1. (b) McIntosh, T. J.; Waldbilling, R. C.; Robertson, J. D. *Ibid.* **1976**, *448*, 15. (c) Kornberg, R. D.; McConnel, H. M. *Biochemistry* **1971**, *10*, 1111.
10. Northrup, S. H.; Curvin, M. S. *J. Phys. Chem.* **1985**, *89*, 4707.
11. Khalatur, P. G.; Pavlov, A. S.; Balabaev, N. K. *Macromol. Chem.* **1987**, *188*, 3029.
12. Pastor, R. W.; Venable, R. M.; Karplus, M. *J. Chem. Phys.* **1988**, *89*, 1112.
13. Quinn, P. J.; Chapman, D. *Crit. Rev. Biochem.* **1980**, *8*, 1.
14. Brown, M. F.; Williams, G. D. *J. Biochem. Biophys. Met.* **1985**, *11*, 71.
15. Milik, M.; Kolinski, A.; Skolnick, J. *J. Chem. Phys.* **1990**, *93*, 4440.
16. Croxton, C. A. *J. Phys.* **1986**, *A19*, 987.
17. Bareman, J. P.; Cardini, C.; Klein, M. *Phys. Rev. Lett.* **1988**, *60*, 2152.
18. Kox, A. J.; Michels, J. P. J.; Wiegel, F. W. *Nature* **1980**, *287*, 317.
19. (a) Colin, D. B.; Barry, T.; Yu-Tai, Tao; Joseph, E.; George, M. W.; Ralph, G. N. *J. Am. Chem. Soc.* **1989**, *111*, 321.
20. Hautman, J.; Klein, M. L. *J. Chem. Phys.* **1989**, *91*, 4994.
21. Hautman, J.; Klein, M. L. *J. Chem. Phys.* **1990**, *93*, 7483.
22. Bareman, J. P.; Klein, M. L. *J. Phys. Chem.* **1990**, *94*, 5202.
23. Karabani, S.; Toxvaerd, S. *J. Chem. Phys.* **1992**, *96*, 5505.
24. Karabani, S.; Toxvaerd, S.; Olsen, O. H. *J. Phys. Chem.* **1992**, *96*, 4965.
25. Shin, S.; Collazo, N.; Rice, S. A. *J. Chem. Phys.* **1992**, *96*, 1352.
26. Shin, S.; Collazo, N.; Rice, S. A. *J. Chem. Phys.* **1993**, *98*, 3469.
27. Shin, S.; Rice, S. A. *Langmuir* **1994**, *10*, 262.
28. Collazo, N.; Shin, S.; Rice, S. A. *J. Chem. Phys.* **1992**, *96*, 4735.
29. Chynoweth, S.; Klomp, U. C.; Michopoulos, Y. *J. Chem. Phys.* **1991**, *95*, 3024.
30. Ryckaert, J.-P.; Bellemans, A. *Faraday Discuss. Chem. Soc.* **1978**, *66*, 95.
31. van der Ploeg, P.; Berendsen, H. J. C. *Mol. Phys.* **1983**, *49*, 233.
32. Chynoweth, S.; Klomp, U. C.; Scales, L. E. *Comput. Phys. Commun.* **1991**, *62*, 297.
33. (a) Evans, D. J.; Hoover, W. G.; Failor, B. H.; Moran, B.; Ladd, A. J. C. *Phys. Rev., A.* **1983**, *28*, 1016. (b) Simmons, A. D.; Cummings, P. T. *Chem. Phys. Lett.* **1986**, *129*, 92.
34. Gear, W. C. *Numerical Initial Value Problems in Ordinary Differential Equations*; McGraw-Hill: New York, 1965.